Published in final edited form as:
Pflugers Arch. 2009 March ; 457(5): 1079–1091. doi:10.1007/s00424-008-0579-1.

Defective jejunal and colonic salt absorption and altered Na^+/H^+ exchanger 3 (NHE3) activity in NHE regulatory factor 1 (NHERF1) adaptor protein-deficient mice

N. Broere,
Department of Biochemistry, Erasmus University Medical Center, Rotterdam 3015GE, The Netherlands

M. Chen,
Department of Gastroenterology, Hepatology and Endocrinology, Hannover Medical School, Carl-Neuberg-Straße 1, Hannover 30625, Germany

A. Cinar,
Department of Gastroenterology, Hepatology and Endocrinology, Hannover Medical School, Carl-Neuberg-Straße 1, Hannover 30625, Germany

A. K. Singh,
Department of Gastroenterology, Hepatology and Endocrinology, Hannover Medical School, Carl-Neuberg-Straße 1, Hannover 30625, Germany

J. Hillesheim,
Department of Gastroenterology, Hepatology and Endocrinology, Hannover Medical School, Carl-Neuberg-Straße 1, Hannover 30625, Germany

B. Riederer,
Department of Gastroenterology, Hepatology and Endocrinology, Hannover Medical School, Carl-Neuberg-Straße 1, Hannover 30625, Germany

M. Lünnemann,
Department of Gastroenterology, Hepatology and Endocrinology, Hannover Medical School, Carl-Neuberg-Straße 1, Hannover 30625, Germany

I. Rottinghaus,
Department of Gastroenterology, Hepatology and Endocrinology, Hannover Medical School, Carl-Neuberg-Straße 1, Hannover 30625, Germany

A. Krabbenhöft,
Department of Gastroenterology, Hepatology and Endocrinology, Hannover Medical School, Carl-Neuberg-Straße 1, Hannover 30625, Germany

R. Engelhardt,
Department of Gastroenterology, Hepatology and Endocrinology, Hannover Medical School, Carl-Neuberg-Straße 1, Hannover 30625, Germany

B. Rausch,
Department of Gastroenterology, Hepatology and Endocrinology, Hannover Medical School, Carl-Neuberg-Straße 1, Hannover 30625, Germany

Correspondence to: U. Seidler, Seidler.Ursula@#mh-hannover.de.

E. J. Weinman,
Departments of Medicine and Physiology, School of Medicine, University of Maryland, Baltimore, MD 21201, USA

M. Donowitz,
Departments of Medicine and Physiology, School of Medicine, Johns Hopkins University, Baltimore, MD 21205-2195, USA

A. Hubbard,
Departement of Cell Biology, School of Medicine, Johns Hopkins University, Baltimore, MD 21205-2195, USA

O. Kocher,
Department of Pathology, Beth Israel Deaconess Medical Center and Harvard Medical School, Boston, MA 02215, USA

H. R. de Jonge,
Department of Biochemistry, Erasmus University Medical Center, Rotterdam 3015GE, The Netherlands

B. M. Hogema, and
Department of Biochemistry, Erasmus University Medical Center, Rotterdam 3015GE, The Netherlands

U. Seidler
Department of Gastroenterology, Hepatology and Endocrinology, Hannover Medical School, Carl-Neuberg-Straße 1, Hannover 30625, Germany

U. Seidler: Seidler.Ursula@#mh-hannover.de

Abstract

We investigated the role of the Na^+/H^+ exchanger regulatory factor 1 (NHERF1) on intestinal salt and water absorption, brush border membrane (BBM) morphology, and on the NHE3 mRNA expression, protein abundance, and transport activity in the murine intestine. NHERF1-deficient mice displayed reduced jejunal fluid absorption in vivo, as well as an attenuated in vitro Na^+ absorption in isolated jejunal and colonic, but not of ileal, mucosa. However, cAMP-mediated inhibition of both parameters remained intact. Acid-activated NHE3 transport rate was reduced in surface colonocytes, while its inhibition by cAMP and cGMP was normal. Immunodetection of NHE3 revealed normal NHE3 localization in the BBM of NHERF1 null mice, but NHE3 abundance, as measured by Western blot, was significantly reduced in isolated BBM from the small and large intestines. Furthermore, the microvilli in the proximal colon, but not in the small intestine, were significantly shorter in NHERF1 null mice. Additional knockout of PDZK1 (NHERF3), another member of the NHERF family of adaptor proteins, which binds to both NHE3 and NHERF1, further reduced basal NHE3 activity and caused complete loss of cAMP-mediated NHE3 inhibition. An activator of the exchange protein activated by cAMP (EPAC) had no effect on jejunal fluid absorption in vivo, but slightly inhibited NHE3 activity in surface colonocytes in vitro. In conclusion, NHERF1 has segment-specific effects on intestinal salt absorption, NHE3 transport rates, and NHE3 membrane abundance without affecting mRNA levels. However, unlike PDZK1, NHERF1 is not required for NHE3 regulation by cyclic nucleotides.

Keywords

PDZ domain proteins; Intestinal electrolyte transport; PDZK1; NHERF1; EPAC; Knockout mice

Introduction

Electroneutral NaCl absorption is the major mechanism for intestinal salt and water absorption and is primarily mediated via the Na^+/H^+ exchanger NHE3 [25] in conjunction with the Cl^-/HCO_3^- exchangers DRA (Slc26a3) [26] and PAT1 (Slc26a6) [27]. The agonist-induced inhibition of this transport process causes diarrhea and is operative in diarrheal diseases of most etiologies. An increase in the enterocyte intracellular cyclic nucleotide levels, elicited by multiple enterotoxins, hormones, and paracrine mediators, inhibits intestinal fluid absorption in vivo [10], and sodium as well as chloride absorption in isolated small and large intestinal mucosa in vitro in the presence but not in the absence of NHE3 [27]. NHE3-binding proteins were identified as cofactors required for cAMP-mediated inhibition and were later called NHERF1 (EBP50) and NHERF2 (E3KARP) (reviewed in [9, 17]). It was shown that cAMP-mediated inhibition of NHE3 expressed in PS120 fibro-blasts required coexpression of either NHERF1 or NHERF2, which can both bind to NHE3 with their PDZ protein–protein interaction domains [18, 36].

These early studies were the first steps toward the understanding that NHE3, like many other transport proteins, is regulated within a multiprotein complex containing the ion transporter as well as the anchoring proteins, the cytoskeleton, and the required protein kinases [17, 28, 29]. It has since then been formulated that using drugs to target the PDZ domain interaction could theoretically be a highly efficient antidiarrheal strategy [17, 20]. One cornerstone of future drug development targeting NHERF-mediated protein–protein interactions is an understanding of their function in different tissues of the living organism.

In this study, we examined the effect of NHERF1 ablation on fluid absorption in the intestine in vivo and observed a decreased fluid absorption in the jejunum of NHERF1-deficient mice corresponding to reduced sodium and chloride absorption in isolated jejunal mucosa. Furthermore, we studied the regulation of NHE3 activity in colonic and small intestinal enterocytes of NHERF1-deficient mice and found decreased acid-activated NHE3 transport rates in 2′,7′-bis(2-carboxyethyl)-5(6)-carboxyfluorescein (BCECF)-loaded surface enterocytes, whereas the inhibition of NHE3 transport rates by cyclic nucleotides was still intact in the absence of NHERF1. The amount of NHE3 in the brush border was reduced, but the apical localization of NHE3 was unaffected by NHERF1 ablation. Because PDZK1 (PDZ domain protein kidney 1, also called NHERF3) binds both to NHERF1 and NHE3 [12], we also studied the effect of combined NHERF1 and PDZK1 ablation on intestinal salt and water transport and the regulation of NHE3 transport rates. Absence of both PDZ proteins did not result in further reduction of jejunal fluid absorption or NHE3 abundance in the BBM, but it further reduced basal NHE3 activity in the colon and severely interfered with NHE3 regulation by acid and second messengers.

Materials and methods

Animals

NHERF1 null mice were generated in the laboratory of E.J. Weinman as described [30] and were bred for at least six generations into the FVB/N genetic background in the animal houses of the Erasmus University of Rotterdam and the Hannover Medical School. $PDZK1^{-/-}$ mice were generated in the laboratory of O. Kocher at Harvard Medical School as described [16]. For the purpose of this study, they were crossed into the FVB/N background and bred for several generations, before breeding NHERF1/PDZK1 double-deficient mice. Wild-type (WT) control mice were bred from the same founders. Mice used in experiments were sex- and age-matched, littermates in the case of the single-deficient mice, and no more than two generations apart (same great-grandparents) in the case of the double-deficient mice. Animal experiments followed approved protocols at the Medical

School of Hannover and local authorities for the regulation of animal welfare (Regierungspräsidium) and the Dutch Animal Welfare Committee. Animals had ad libitum access to water and chow, but were fasted overnight before the in vivo perfusion experiments.

Single-pass jejunal and ileal perfusion experiments in vivo

Induction of anesthesia was achieved by the administration of 10 μL/g intraperitoneal (IP) haloperidol/midazolam/fentanyl cocktail (haloperidol 12.5 mg/kg, fentanyl 0.325 mg/kg, and midazolam 5 mg/kg body weight) and maintained using the cocktail at 20% of the initial dose every 30–45 min when necessary, as indicated by respiratory rate and toe pinch reflex. The abdomen was opened by a small central incision, and approximately 10–15 cm of the jejunum or the last part of the ileum, was exposed for the subsequent ligation. A polyethylene tube (PE100) with a distal flange was advanced to the jejunum (first incision 3–4 cm distal to the stomach and a PE200 tube was advanced into the proximal part to allow drainage of proximal secretions, then another PE100 tube was advanced into the midjejunum (6–8 cm distal to pylorus) and secured by a ligature. The 10- to 15-cm isolated jejunal segment with intact blood supply was gently flushed and then perfused (Perfusor compact, BRAUN) at a rate of 3 mL/h with 150 mM NaCl. Effluents from the isolated segment were free of blood (visually and by hemoccult test) throughout all experiments. Perfusion of the ileum was performed in a similar way. Animals were maintained at 37°C using a heating pad controlled by a rectal thermistor probe. After an initial 30-min washout, basal fluid absorption was measured for 30 min, followed by a 30-min perfusion with 150 mM NaCl containing 100 μM forskolin (FSK). At the end, mice were killed by cervical dislocation and the length of the perfused jejunum was measured. The perfusate was collected in a preweighed 4.5-mL collecting tube. The amount of fluid absorbed was calculated by subtracting the amount of fluid recovered after 30 min from the amount perfused during the 30 min (1.5 mL) and absorption rates are expressed in milliliters of fluid absorbed per centimeter jejunum length per hour.

Isolated loop experiments for in vivo measurement of intestinal fluid uptake

Fluid absorption was determined in mice (12–20 weeks) under ketamine/xylazine anesthesia (100 and 20 mg/kg, respectively, IP). An incision was made along the abdominal midline. The small intestine was rinsed with phosphate-buffered saline (PBS; 37°C) through a small distal incision and the proximal part of the jejunum and the ileum were divided in loops (10–12 cm each) which were closed by sutures and filled with isotonic PBS (37°C; approximately 90 μL/cm). The abdomen was closed with clips and animals were placed in a humidified 37°C incubator. After 1 h, mice were euthanized and the loop length and remaining fluid were measured. When indicated, 8-Br-cAMP (2 mM) or 8-Br-cGMP (0.5 mM) was added to the luminal solution; in that case, the experiment was terminated after 2 h instead of 1 h. Absorption was determined as the difference between the amount of fluid injected and the remaining amount of fluid and expressed as milliliters of fluid absorbed per centimeter jejunum length per hour.

$^{22}Na^{+}$ and $^{36}Cl^{-}$ flux studies in isolated mucosa in vitro

The preparation of the isolated jejunal mucosa and the $^{22}Na^{+}$ and $^{36}Cl^{-}$ flux studies were performed under short-circuit conditions exactly as recently described [27]. For the colonic flux measurements, the serosal to mucosal and the mucosal to serosal fluxes were determined in equivalent segments of proximal colon from two different mice because the colon is too short to allow isolation of multiple pieces of tissue.

Preparation of colonic crypts and pH_i measurements

Murine colonic crypt preparation and fluorometric pH measurements were performed exactly as recently described [7]. The principle of the pH_i measurement method is that BCECF-loaded colonic crypts were acidified using an ammonium prepulse (40 mM NH_4Cl isotonically replacing NaCl) for 5 min, then perfused for 5 min with a Na^+-free buffer (TMA^+ isotonically replacing Na^+), until pH_i reached its lowest value plateau. Subsequently, 50 μM HOE642 and, if appropriate, 10^{-5} M FSK was added to the Na^+-free buffer; 50 μM HOE642 has previously been shown to completely inhibit NHE1 and NHE2 [1]. After 2–3 min, the buffer was switched to Na^+-containing buffer, containing 50μM HOE642 and FSK or 8-Br-cGMP, if appropriate. Images were digitized every 1 s (phase of rapid pH_i recovery) to 30 s (plateau phases) with a cooled CCD camera (CoolSnap ES, Roper Scientific, Ottobrunn, Ger-many) using Metafluor software (Universal Imaging, Downington, PA, USA) during exposure of cells to alternating 440 and 495 nm light from a monochromator (Visichrome, Visitron Systems, Puchheim, Germany) with a 515-nm DCXR dichroic mirror and a 535-nm barrier filter (Chroma Technology, Rockingham, VT, USA) in the emission pathway. Calibration of the 440/495 ratio was performed as described previously [2]. Regions of interest (ROIs) were selected in the apical part of the crypts where NHE3 is expressed. Intrinsic buffering capacity (β_i) was determined for isolated murine colonic crypts using the protocol as described by Boyarsky et al. [4]. β_i did not differ significantly between a variety of mouse genotypes and transgenes [2, 3, 7] and has been published in graphic form before [2].

Immunohistochemistry and confocal microscopy

Formalin-fixed, paraffin-embedded tissue sections (5 μm) from mice with different genotypes were prepared on the same slide. After deparaffinization with xylene and treatment with 0.01 M sodium citrate solutions, endogenous peroxidase activity was blocked with 0.6% H_2O_2 and 0.12% sodium azide. Sections were incubated with anti-NHE3 antibodies (1:100; NHE31-A, Alpha Diagnostics) in PBS with 2% bovine albumin for 1 h at room temperature. Sections were subsequently incubated for 2 h with fluorescein isothiocyanate-labeled secondary antibody (1:100; Nordic) and mounted with Vectashield (Vector). Immunofluorescence micrographs were captured using a Zeiss LSM510 confocal microscope equipped with a 25-mW argon laser (488 nm). Fluorescence emission after excitation at 488 nm was detected using a ×40/1.3 numerical aperture oil immersion lens, a dichroic beam splitter reflecting 488 nm excitation light, and a 505–530 bandpass emission filter. Images were scanned using a 428-μm (colon) and 703-μm (jejunum) pinhole size. The same threshold was utilized for all images from one slide. Several sections were analyzed from three age- and sex-matched mice of each genotype.

Preparation of jejunal and colonic brush border membranes and Western blot analysis

NHE3 quantification was performed both in Hannover and in Rotterdam, using similar procedures. For Western blotting, epithelial cells lysates were obtained after mechanical vibration (small intestine) or scraping (colon) and BBM vesicles were purified by divalent cation precipitation and used for Western blotting exactly as recently described [5, 14].

Quantitative RT-PCR

Polymerase chain reaction (PCR) primers were designed using the computer programs “HUSAR PRIME” Sequence Analysis Software (STZ Genominformatik, Heidelberg) or with “Primer Express” (Applied Biosystems). Primer sequences were NHE3.for: 5′-AGGCCACCAACTATGAA-GAG-3′, NHE3.rev: 5′-AGGGGAGAACAC-GGGATTATC-3′, PCR product length 110 bp, (NHE3, NM_00108160); villin.for: 5′-TCATACTCA AGACTCCGTCC-3′; villin.rev:5-TACCACTTGTTTCTCC GTCC-3′; 119

bp; (Villin1, NM_009509.1); RPS9.for: 5′-AA GCACATCGACTTCTCCC-3′; RPS9.rev: 5′-ACAATC CTCCAGTTCAGCC-3′, 150 bp; RPS9 (ribosomal protein 9, NM_ 029767.2). Real-time polymerase chain reactions (RT-PCR) were carried out using SyberGreen PCR-Master-Mix (Applied Biosystems) in the Applied Biosystems 7300 Real-time PCR System. PCR extension was performed at 60°C with 40 repeats. Data were analyzed using Sequence Detection Software 1.2.3 (Applied Biosystems) and exported to Microsoft Excel. Relative quantification was carried out using Villin and RPS9 as reference genes.

Electron microscopy

Electron microscopical analysis of samples from the proximal colon, jejunum, and ileum was performed exactly as described [22]. The average microvillar length was determined by calculating the average length from several individual microvilli from at least 20 cells from each sample at a ×25,000 magnification. Samples from three mice of each genotype were analyzed.

Statistical analyses

Values are expressed as the mean±SE. Statistical analysis was performed using Student's *t* test, Wilcoxon rank test, or analysis of variance. p values <0.05 were considered statistically significant.

Results

In vivo fluid absorption rates in the NHERF1$^{-/-}$ and NHERF1$^{+/+}$ murine jejunum and ileum during single-pass perfusion

Basal fluid absorption rates in the midjejunum of anesthetized mice were significantly lower in NHERF1$^{-/-}$mice compared with WT littermates (Fig. 1a). Since fluid movement is secondary to electrolyte movements, this suggests that net salt absorption is reduced in the jejunum in the absence of NHERF1. Subsequent addition of 10^{-4} M FSK to the luminal perfusate induced fluid secretion in both NHERF1$^{-/-}$ mice and control littermates, but the effect of FSK addition was significantly lower in NHERF1$^{-/-}$ mice compared with NHERF1$^{+/+}$ littermates. In contrast, no significant difference in fluid absorption was observed in the distal ileum of NHERF1-deficient mice (Fig. 1b). In the proximal colon, similar experiments were not successful because the colonic mucosa secreted fluid even in what we measure as the "basal period." We assume that the manipulation of the proximal colon to empty its fecal content elicits long-lasting secretory reflexes.

Because the changes in fluid flux are generated both by an inhibition of salt absorption and a stimulation of anion secretion, primarily through the cystic fibrosis transmembrane conductance regulator (CFTR) chloride channel which is also regulated by NHERF1, it cannot be said with certainty which process is primarily affected. This was clarified by performing isotope flux studies in isolated jejunal mucosa in an Ussing chamber setup.

$^{22}Na^{+}$ and $^{36}Cl^{-}$ fluxes in isolated jejunal and colonic mucosa of NHERF1$^{-/-}$ and WT mice

Net Na^{+} and Cl^{-}absorption was measured in isolated jejunal mucosa by assessing bidirectional $^{22}Na^{+}$ and $^{36}Cl^{-}$ fluxes and subtracting the mucosal to serosal flux from the serosal to mucosal flux for each individual tissue pair. Basal net Na^{+} absorption was significantly decreased in NHERF1$^{-/-}$jejuna compared with WT controls, but the inhibition by FSK was intact in the absence of NHERF1. In addition, stimulation of the Na^{+}/glucose cotransporter by addition of luminal glucose resulted in comparable increases in sodium flux (as well as the short-circuit current), indicating that sodium-coupled glucose cotransport is unaffected by the absence of NHERF1 (Fig. 2a).

The net Cl^- absorption was also reduced in the absence of NHERF1 (Fig. 2b). Furthermore, the FSK-stimulated net Cl^- secretion was significantly lower in the NHERF1 null mice, in contrast to the normal efficacy of cAMP in inhibiting Na^+ absorption. This corresponded to a strong reduction in the FSK-stimulated short-circuit current in the NHERF1$^{-/-}$ tissues compared with the WT tissues (ΔI_{sc} was 195±26 μA/cm^2 in WT vs. 102±12 μA/cm^2 in NHERF1-deficient jejunal mucosa), as has been observed in NHERF1$^{-/-}$ mice before [5]. Together, the results suggest that the absence of NHERF1 causes a significant reduction in the basal Na^+ absorption and reduced cAMP-mediated stimulation of CFTR-dependent anion secretion, but does not significantly affect cAMP-mediated inhibition of NHE3-dependent jejunal salt absorption.

The same experiments were performed in isolated proximal colonic mucosa. Because of the small size of the proximal colon, proximal colon sections from two different mice were used to determine the unidirectional fluxes. Again, the net Na^+ absorption rates were mildly but significantly reduced in the NHERF1$^{-/-}$ mucosa, and inhibition by cAMP was observed (Fig. 3). Because of the small size of the proximal colon and the necessity to perform many flux experiments to obtain significant results, we did not perform Cl^- fluxes.

Segment-specific changes in fluid absorption assessed by ligated loop experiments

In addition to the single-pass perfusion experiments, the ligated loop technique was used for assessing fluid movements in the intestine in vivo. With this method, fluid movement can be determined in different segments of the small intestine simultaneously. There was a significant difference in basal fluid absorption between NHERF1-deficient jejunum, but not in the ileum (Fig. 4). Inhibition of fluid absorption by cyclic nucleotides was assessed by adding 8-Br-cAMP or 8-Br-cGMP. The cyclic nucleotide-dependent inhibition of fluid absorption in the NHERF1-deficient mice was significantly reduced in the jejunum but not in the ileum. The effect of 8-Br-cAMP was less than the effect of FSK (Fig. 1), and cGMP-dependent inhibition was not as pronounced as cAMP-mediated inhibition. Although the fluid absorption rate after the addition of 8-Br-cGMP was similar in WT and NHERF1 null mice, the percentage inhibition by 8-Br-cGMP was significantly reduced from 57% to 45% in NHERF1 null mice. These results confirm the findings from the single-pass perfusion experiments, and the lack of effect of NHERF1 ablation in the ileum correlates with the finding that CFTR activation was reduced in NHERF1-deficient jejunum but not in the ileum [5].

NHE3 transport activity in surface colonocytes from NHERF1$^{-/-}$ and NHERF1$^{+/+}$ intestine

In order to quantify NHE3 exchange activity in native NHE3-expressing enterocytes, we loaded isolated colonic crypts with the pH-sensitive dye BCECF and measured the acid-activated Na^+-dependent proton flux in the upper part of the glands in the presence of 50 μM HOE642. At this concentration, HOE642 inhibits NHE1 and NHE2 but not NHE3 activity [1]. In NHE3-deficient colonic crypts, the acid-activated, Na^+-dependent, HOE642-insensitive proton fluxes was found to be reduced by approximately 85% in a previous study [7], validating the method for the measurement of NHE3 activity in native enterocytes. In the apical region of NHERF1$^{-/-}$ crypts, the acid-activated, HOE642-insensitive Na^+-dependent proton flux was diminished by 30% compared with NHERF1$^{+/+}$ crypts (Fig. 5a). This difference was abolished after treatment with 10^{-5} M of the NHE3-specific inhibitor S1611, indicating that it is due to a difference in NHE3 activity. In the presence of S1611, 10^{-5} M FSK had no further inhibitory effect, suggesting that NHE3 is the target for cAMP-dependent inhibition of the acid-activated, HOE642-insensitive Na^+-dependent proton flux.

In order to study the regulation of NHE3 in NHERF1-deficient colonocytes, we measured the acid-activated, HOE642-insensitive Na^+-dependent proton flux in NHERF1$^{-/-}$ and

NHERF1$^{+/+}$ surface colonocytes in the absence and presence of 10^{-5} M FSK or 10^{-3} M 8-Br-cGMP (both at maximal inhibitory concentrations which were determined in experiments not shown). There was significant inhibition by both compounds in NHERF1$^{-/-}$ as well as NHERF1$^{+/+}$ crypts (Fig. 5b), although the percentage of inhibition was slightly but significantly reduced in the NHERF1$^{-/-}$ mice ($p<0.05$). It should be noted, however, that the proton flux in NHE3 null mice was still approximately 4 mM/min [7] and was not fully inhibited by S1611 (Fig. 5a). Therefore, the difference between NHERF1$^{+/+}$ and NHERF1$^{-/-}$ mice with respect to the cAMP or cGMP-dependent inhibition of the acid-stimulated proton flux was less prominent if corrected for this NHE3-independent part of the proton flux.

Effect of EPAC activation on fluid absorption and NHE3 activity

It was recently shown that in addition to protein kinase A (PKA), the exchange protein activated by cAMP (EPAC) can also cause cAMP-mediated inhibition of NHE3 in the proximal tubule of the kidney in a NHERF1-dependent manner [15, 22]. This protein is also expressed in the intestine [22]. We investigated whether EPAC activation results in changes in ion and fluid transport in the jejunum. In contrast to the PKA activator 8-pCPT-cAMP, which caused a dramatic decrease in fluid absorption (Fig. 6a), addition of 200 μM of the structurally very similar but highly selective EPAC activator 8-pCPT-2′-*O*-Me-cAMP did not result in a significant change in fluid absorption. This suggests that the pathway of NHE3 inhibition or CFTR activation via EPAC plays no role in the jejunum. We also tested the effect of EPAC activation on NHE3 activity in the surface cells of isolated colonic crypts (Fig. 6b). In this segment, addition of the EPAC activator 8-pCPT-2′-*O*-Me-cAMP (100 μM) caused a slight but significant inhibition of acid-activated NHE3 activity in NHERF1$^{+/+}$ surface cells, whereas 10^{-5} M FSK caused a much stronger inhibition. Together, this indicates that EPAC is not a major pathway in the cAMP-mediated regulation of NHE3 in the intestine and that the NHERF1 dependency of EPAC-mediated NHE3 inhibition, as observed in the proximal tubule [22], can only play a minor role in the colon.

Western blot analysis of BBM from the small intestine and colon of NHERF1-deficient mice and WT littermates

In order to search for the molecular mechanism causing the reduced sodium absorption and acid-activated NHE3 transport rate, we isolated brush border membranes (BBM) from the small and large intestine and studied NHE3 abundance by Western blot analysis. NHE3 abundance was significantly reduced (approximately 40%) in the BBM but not in the total cell lysate of small intestinal cells (Fig. 7a). Several aspecific bands were detected by the antibody that were mostly absent from the purified brush borders. Use of a blocking peptide or boiling the samples (which is known to precipitate NHE3) resulted in absence of the band representing NHE3 (indicated in the figure) without any effect on the other bands (data not shown). Similar results were obtained in colon, although the reduction in NHE3 abundance in the apical membranes was smaller than in the small intestine (Fig. 7b).

Immunohistochemical staining and mRNA expression levels of NHE3 in the small and large intestine in NHERF1$^{+/+}$ and NHERF1$^{-/-}$ mice

Immunohistochemical detection of NHE3 by confocal microscopy revealed a strong apical staining in small intestinal villus cells and colonic surface cells from both WT and NHERF1-deficient mice (Fig. 8). We observed a rather large variability of NHE3 staining in immunohistochemical experiments. Because of the lack of suitable control proteins to use for standardization, we, therefore, used immunohistochemistry in a qualitative fashion only to assess the cellular localization NHE3. All detectable NHE3 was present in the apical region of the cells, and no redistribution of NHE3 into other cellular compartments was detected using these methods in the NHERF1 null mice.

NHE3 mRNA was measured by a quantitative PCR protocol using the villin gene as internal control. No significant change in NHE3 mRNA levels was detected in small and large intestinal epithelium of NHERF1$^{-/-}$ mice compared with WT littermates. Villin mRNA expression was not altered in the NHERF1$^{-/-}$ mice, when compared to the ribosomal protein RPS9 (Fig. 9a, b).

Electron microscopy

Analysis of the ultrastructure of the apical border of enterocytes was performed by electron microscopy. No changes in the length or ultrastructure of the microvilli were observed in the jejunal sections (Fig. 10a). In contrast, the length of the colonic microvilli was significantly reduced by approximately 35% in the NHERF1 null mice (Fig. 10b, c). They also appeared to be stubbier than the microvilli from WT mice.

Effect of NHERF1/PDZK1 double deficiency on jejunal fluid absorption

In addition to NHERF1, additional members of the NHERF family of proteins are known to be involved in the regulation of NHE3. In order to determine whether effects of NHERF1 and PDZK1 ablation are additive, fluid absorption was determined in NHERF1/PDZK1 double-deficient mice and compared with respective WT mice derived from the same founders and from the same generation (second cousins). The reduction in jejunal fluid absorption was similar to that observed in the NHERF1 null mice (Fig. 11a), and no significant further reduction in BBM NHE3 abundance was observed compared with the NHERF1-deficient mice (data not shown).

NHE3 activity and regulation in NHERF1/PDZK1 double-deficient colonic surface cells

In contrast to the jejunal fluid absorption, the acid-activated NHE3 activity in colonic surface cells from NHERF1/PDZK1 double-deficient mice was strongly reduced, and the NHE3 inhibition by FSK was completely abolished. Thus, double-deficient mice show a combination of the defects observed in NHERF1$^{-/-}$ mice (this paper) and the defects related to NHE3 transport rate regulation in PDZK1$^{-/-}$ intestine reported previously [14].

Discussion

This work investigates the role of the NHE3-binding PDZ domain protein NHERF1 in intestinal fluid and electrolyte absorption and studies the molecular mechanisms responsible for the observed reduced absorptive rates. In the absence of NHERF1, jejunal, but not ileal, fluid absorption was significantly reduced in vivo, and the magnitude of change from absorption to secretion after the application of luminal FSK was significantly diminished. While the reduced CFTR activation in the absence of NHERF1 [5] can explain the latter observation, it cannot explain the former. Therefore, Na^+ and Cl^- transport was measured in isolated jejunal and colonic mucosa in vitro. Basal jejunal and colonic Na^+ absorptive rates were found to be significantly reduced with intact inhibition of absorption by a rise in intracellular cAMP levels (Fig. 2). In addition, acid-activated NHE3 transport rates were significantly reduced in colonic surface cells, but the inhibition of NHE3 activity by cyclic nucleotides was preserved. Western blot analysis revealed a reduction in the abundance of NHE3 in the jejunal and colonic BBM, and electron microscopy revealed significantly shortened microvilli in the proximal colon of NHERF1 null mice. Additional deficiency of PDZK1 abolished NHE3 inhibition by cAMP without a further reduction in NHE3 BBM abundance or jejunal fluid absorption compared with NHERF1 null mice. Taken together, the results demonstrate an important, but segment-specific role for NHERF1 in intestinal NHE3 membrane abundance, but no crucial role for the cAMP-dependent regulation of intestinal NHE3 activity.

NHERF1 was the first PDZ domain adaptor protein identified through its binding to NHE3 in the proximal tubule [31, 33]. It enhanced the inhibitory effect of PKA on NHE3 in isolated renal BBM [32, 33] and established an inhibitory effect of cAMP on NHE3 when both proteins were coexpressed in PS120 and Caco-2 fibroblasts [18, 34, 36]. Recently, mice have been generated that lack the expression of NHERF1 [21, 30], NHERF2 [5], or PDZK1 (NHERF3) [16], another PDZ protein that binds to NHE3 [12]. NHERF1 null mice display a surprising variability in the phenotype in different tissues, and the current study demonstrates that NHERF1 ablation even affects salt and fluid transport and NHE3 activity differently in various segments of the intestine. In isolated proximal tubules, NHE3 inhibition by cAMP was abolished in NHERF1-deficient mice, which was explained by loss of cAMP-dependent phosphorylation of NHE3 [22, 32]. In contrast, basal NHE3 activity as well as inhibition by 8-Br-cAMP was unaltered in ileal villi of NHERF1-deficient mice [22]. This was extended by our observation that basal and cAMP-inhibited fluid absorption rates are normal in the ileum of NHERF1-deficient mice. Absence of NHERF3 (PDZK1), unexpectedly, resulted in reduction of jejunal Na^+ absorption and strong attenuation of its inhibition by an increase in intracellular cAMP [14], as well as abrogation of cAMP-mediated NHE3 inhibition in the large intestine [7], although PDZK1 is expressed at lower levels than NHERF1 in this tissue [14]. Loss of NHERF2, which is also expressed in the intestine and can substitute for NHERF1 in PS120 fibroblasts with respect to cAMP-mediated inhibition of NHE3, did not impede cAMP-mediated NHE3 inhibition in enterocytes, although it did abolish Ca^{2+}-mediated inhibition [17], a feature also previously recognized in NHE3-transfected PS120 fibro-blasts [19].

These results demonstrated that despite high structural homology within their PDZ domains, the biological functions of the three NHERF proteins are unique. In addition, the data are explicable only when accepting the hypothesis that for each transporter, the multiprotein complexes which mediate a similar function, i.e., cAMP-mediated inhibition of NHE3, are likely to be composed of different components in different epithelia. Thus far, much attention has been paid to the role of the PKA-anchoring protein ezrin in NHE3 inhibition. The formation of a complex containing NHE3, NHERF1, ezrin, and PKA appears crucial for cAMP-dependent inhibition of NHE3 in PS120 fibroblasts [18]. In the proximal tubule, the affinity of PDZK1, another NHE3-binding PDZ protein, for the kinase-anchoring protein D-AKAP-II was higher than its affinity for the kinase-anchoring protein ezrin, suggesting that differences in the components of a multiprotein complex may be found at many levels [11]. One conclusion from these observations was that more studies in native systems are required to better delineate the physiological significance of the NHERF adaptor proteins in the regulation of ion transport in the different organ systems [8, 17, 35].

A first glimpse into this complexity was recently provided by the demonstration that, in the kidney, an additional pathway exists for cAMP-mediated inhibition of NHE3 to the PKA-mediated phosphorylation, mediated by the exchange protein activated by cAMP (EPAC) [15, 22] and that inhibition of NHE3 by both mechanisms was abolished in the kidney of NHERF1 null mice [22]. Since the protein EPAC is also expressed in the small and large intestinal mucosa, we tested the effect of EPAC activation on fluid movements in the jejunum and NHE3 regulation in colonic surface cells. The EPAC activator 8-pCPT-2′-*O*-Me-cAMP did not significantly affect jejunal fluid absorption. However, NHE3 activity was slightly but significantly inhibited in surface colonocytes (Fig. 6b). Considering that NHERF1 ablation has been shown to attenuate EPAC-dependent inhibition of NHE3 in the kidney, the reduced inhibition of NHE3 activity by FSK in NHERF1-deficient colonocytes (Fig. 5) may in part be caused by loss of EPAC-dependent inhibition. As the contribution of EPAC activation in relation to the overall effect of an increase in cAMP levels was small even in these cells, we did not attempt to prove this hypothesis. Why EPAC activation has

different effects on renal, colonic, and small intestinal NHE3 is unclear at this time. In fact, the molecular mechanism by which EPAC affects NHE3 has not been elucidated yet.

Our study suggests that NHERF1 is required for optimal BBM expression of NHE3 in enterocytes from small and large intestine. The abundance of NHE3 was reduced relative to β-actin, a major component of the subapical cytoskeletal network, and also relative to the structural BBM protein villin (data not shown). Immunohistochemical staining of NHE3 located the protein only in the brush border both in WT and NHERF1 null mice. The variability of the staining of tissue from different animals was relatively large and, although we used it only in a qualitative fashion, there was a trend toward lower signal intensity in the NHERF1 null mice without any effect on the subcellular localization at the resolution obtained by confocal microscopy. Taken together, the decreased NHE3 membrane abundance seems the best explanation for the significantly reduced fluid absorptive rates in the jejunum and significant reductions in jejunal and proximal colonic net Na^+ absorptive rates. In line with this, no changes in fluid absorption (Fig. 1 and 3) and NHE3 activity [22] were observed in the ileum of NHERF1-deficient mice, which correlates with unaltered NHE3 abundance in the ileal brush border as determined by Western blotting [22]. However, more work at the molecular level is needed to fully understand the changes in NHE3 activity caused by the absence of NHERF1.

In another line of NHERF1 null mice generated by Morales et al., the microvillar structure in the ileum was severely affected [21] with a strong reduction in the number and length of the microvilli, altered cell shape, and dispersed terminal webs. No such effects were previously observed in ileal enterocytes of the $NHERF1^{-/-}$ mouse line used in the current study, which for those experiments was bred into the same C57/Bl6 genetic background used by Morales et al. [22]. For the current study, we analyzed sections from different parts of the intestine from $NHERF1^{-/-}$ mice (from the FVB background) and observed no alterations in microvillar length or the number of microvilli per cell in the jejunum (Fig. 10) and ileum (data not shown). However, microvilli in the proximal colon were significantly shorter in NHERF1 null mice (Fig. 10), and this was also noted in NHERF1 null mice from the C57/Bl6 background (data not shown). Apparently, NHERF1 affects the microvillar ultrastructure in some but not all cases. Two currently known mechanisms could potentially contribute to these alterations. Firstly, the microvilli of enterocytes in ezrin-deficient mice were shorter and thicker than normal [24], and the amount of ezrin (and in particular phosphoezrin) was reduced in the small intestine of NHERF1 null mice [21]. The latter was confirmed by Western blotting of ileal cell scrapings and purified jejunal BBM (M. Donowitz, unpublished observations). Secondly, the GTPase-activating protein EPI64 (EBP50-PDZ interactor of 64 kDa), which was first identified as a NHERF1-interacting protein with a Tre-2/Bub2/Cdc16 (TBC) domain, was shown to be required for microvillus formation in JEG-3 cells, and the interaction with NHERF1 was essential for this. Mutating both the PDZ-interacting motif of EPI64 or knockdown of NHERF1 expression using siRNA resulted in loss of microvilli in cell culture [13]. Involvement of NHERF1 in microvillus formation was also noted in a study in which NHERF1 expression was shown to be induced by the hepatocyte nuclear factor 4α, resulting in microvillus morphogenesis [6]. Clearly, more detailed investigations will be required to clarify why NHERF ablation affects microvillus formation differently in the two lines of NHERF1 null mice and what mechanism(s) cause the reduced microvillar length in the proximal colon.

PDZK1-deficient mice display very different effects on NHE3 compared with NHERF1 null mice, namely, a strong reduction in acid activation of NHE3 transport rate as well as loss of inhibition by an elevation of cAMP or Ca^{2+} in colonic surface enterocytes, although NHE3 protein levels in the BBM were normal [7, 14]. A molecular explanation for these findings, based on heterologous expression studies, is lacking. However, PDZK1-deficient mice

displayed a strong increase in NHE3 mRNA expression levels in small and large intestine, suggesting that the turnover of NHE3 may be dramatically increased in the absence of PDZK1, even though we did not find evidence for a reduction in the amount of NHE3 protein present in the enterocyte cytoplasm or BBM [7, 14]. Because PDZK1 binds to both NHE3 and NHERF1, we wondered whether the combined ablation of NHERF1 and PDZK1 would result in a potentiation of the defects observed in the single null mice. Surprisingly, we observed no further reduction in BBM NHE3 abundance and no further reduction in basal fluid absorption in the jejunum in vivo. However, NHE3 regulation in surface colonic enterocytes of NHERF1/PDZK1 double-deficient mice was drastically changed compared with NHERF1-deficient colonic enterocytes with a strong reduction of acid-activated NHE3 transport rates and a loss of cAMP-mediated inhibition of this acid-activated NHE3 rate. The severe reduction of acid-activated NHE3 activity and the lack of its inhibition by cAMP was identical in colonic surface enterocytes of the NHERF1/PDZK1-deficient and the PDZK1-deficient mouse [7].

In comparison with PDZK1-deficient mice [7, 14], NHERF1-deficient mice displayed a much higher acid-activated NHE3 transport rate in colonic surface cells and preserved regulation by cyclic nucleotides even in those segments of the intestinal tract where Na^+ absorption is affected (jejunum, colon). This may be one reason why the NHE3 mRNA upregulation that occurs in PDZK1 null mice was not observed in the small or large intestine of NHERF1-deficient mice. Another reason may be the simultaneous reduction in CFTR-dependent anion secretion in the absence of NHERF1 [5], which is also seen in vivo (this study). Possibly, the decreased fluid secretion and decrease in absorption results in a balanced state. It will be important in future studies to assess the NHE3 membrane retention time in the absence of the different NHERF proteins and its potential effects on NHE3 regulation.

In summary, our results show that the absence of NHERF1 results in segment-specific changes in intestinal salt absorption in vivo, correlating to a reduced Na^+ absorption in the isolated mucosa of these segments in vitro. In the colon, a correlation between this reduction in electroneutral Na^+ absorption and acid-activated NHE3 transport rates in the surface enterocytes was demonstrated. The membrane abundance of NHE3 was also reduced in the segments that displayed reduced absorptive rates, suggesting a causal relationship. The reduced NHE3 abundance in the proximal colon also correlates with the observed reduction in microvillar length. In contrast to the deletion of PDZK1, intestinal NHERF1 ablation leaves NHE3 regulation by cyclic nucleotides intact. Thus, both NHERF1 and, as shown elsewhere, PDZK1 [14] appear to affect intestinal NHE3 BBM targeting and/or anchoring and both are required for normal intestinal salt and fluid absorptive rates, but the effect of deleting either gene has quite different effects on several aspects of NHE3 regulation in the native intestine. Various factors could potentially explain the difference in function of these two structurally related PDZ adaptors in the native intestine. These include differences between the structure of PDZK1 and NHERF1 (no ERM-binding domain in PDZK1 and more PDZ domains in PDZK1 [17], potentially assembling more binding partners); better preferential binding of Slc26a3, a major partner of NHE3 in salt absorption, to PDZK1 rather than NHERF1 [23]; different expression levels of PDZK1 and NHERF1 in the various intestinal segments [14]; and possibly also differences in protein levels along the crypt-villus axis, which could affect regulation of both NHE3 and CFTR which are mostly localized in the villus and the crypt cells, respectively. Clearly, more detailed studies will be required to gain a full understanding and appreciation of the complexity of regulation of ion transport by the different NHERF proteins, and working models on the regulation of NHE3 membrane anchoring and activity regulation derived from heterologous expression models will be helpful guidelines to design these future experiments. Our studies suggest that the reduction in basal NHE3 activity observed in the jejunum and colon of $NHERF1^{-/-}$ mice, as

well as the lack of changes of fluid transport in the ileum may become an obstacle in using NHERF1 as a target for antidiarrheal action.

Acknowledgments

This work was supported by the Deutsche Forschungsgemeinschaft SFB621/C9, the Lower Saxony Ministry of Science and Education, the Volkswagen Stiftung, and the Dutch Stomach–Liver–Intestine Foundation (MLDS, grant MWO 03-15). A part of this work was prepared in fulfillment with the requirements for the doctoral theses by Nellie Broere, Mingmin Chen, Anurag Singh, and Jutta Hillesheim.

References

1. Bachmann O, Riederer B, Rossmann H, Groos S, Schultheis PJ, Shull GE, Gregor M, Manns MP, Seidler U. The Na^+/H^+ exchanger isoform 2 is the predominant NHE isoform in murine colonic crypts and its lack causes NHE3 upregulation. Am J Physiol Gastrointest Liver Physiol. 2004; 287:G125–G133. [PubMed: 14962844]
2. Bachmann O, Rossmann H, Berger UV, Colledge WH, Ratcliff R, Evans MJ, Gregor M, Seidler U. cAMP-mediated regulation of murine intestinal/pancreatic $Na^+/HCO3^-$ cotransporter subtype pNBC1. Am J Physiol Gastrointest Liver Physiol. 2003; 284:G37–G45. [PubMed: 12388213]
3. Bachmann O, Wuchner K, Rossmann H, Leipziger J, Osikowska B, Colledge WH, Ratcliff R, Evans MJ, Gregor M, Seidler U. Expression and regulation of the $Na^+–K^+–2Cl^-$ cotrans-porter NKCC1 in the normal and CFTR-deficient murine colon. J Physiol. 2003; 549:525–536. [PubMed: 12692180]
4. Boyarsky G, Ganz MB, Sterzel RB, Boron WF. pH regulation in single glomerular mesangial cells. I. Acid extrusion in absence and presence of $HCO3^-$. Am J Physiol. 1988; 255:C844–C856. [PubMed: 2849306]
5. Broere N, Hillesheim J, Tuo B, Jorna H, Houtsmuller AB, Shenolikar S, Weinman EJ, Donowitz M, Seidler U, de Jonge HR, Hogema BM. Cystic fibrosis transmembrane conductance regulator activation is reduced in the small intestine of Na^+/H^+ exchanger 3 regulatory factor 1 (NHERF-1) but not NHERF-2-deficient mice. J Biol Chem. 2007; 282:37575–37584. [PubMed: 17947234]
6. Chiba H, Sakai N, Murata M, Osanai M, Ninomiya T, Kojima T, Sawada N. The nuclear receptor hepatocyte nuclear factor 4alpha acts as a morphogen to induce the formation of microvilli. J Cell Biol. 2006; 175:971–980. [PubMed: 17178913]
7. Cinar A, Chen M, Riederer B, Bachmann O, Wiemann M, Manns M, Kocher O, Seidler U. NHE3 inhibition by cAMP and Ca^{2+} is abolished in PDZ-domain protein PDZK1-deficient murine enterocytes. J Physiol. 2007; 581:1235–1246. [PubMed: 17395628]
8. Donowitz M, Cha B, Zachos NC, Brett CL, Sharma A, Tse CM, Li X. NHERF family and NHE3 regulation. J Physiol. 2005; 567:3–11. [PubMed: 15905209]
9. Donowitz M, Li X. Regulatory binding partners and complexes of NHE3. Physiol Rev. 2007; 87:825–872. [PubMed: 17615390]
10. Field M. Intestinal ion transport and the pathophysiology of diarrhea. J Clin Invest. 2003; 111:931–943. [PubMed: 12671039]
11. Gisler SM, Madjdpour C, Bacic D, Pribanic S, Taylor SS, Biber J, Murer H. PDZK1: II. an anchoring site for the PKA-binding protein D-AKAP2 in renal proximal tubular cells. Kidney Int. 2003; 64:1746–1754. [PubMed: 14531807]
12. Gisler SM, Pribanic S, Bacic D, Forrer P, Gantenbein A, Sabourin LA, Tsuji A, Zhao ZS, Manser E, Biber J, Murer H. PDZK1: I. a major scaffolder in brush borders of proximal tubular cells. Kidney Int. 2003; 64:1733–1745. [PubMed: 14531806]
13. Hanono A, Garbett D, Reczek D, Chambers DN, Bretscher A. EPI64 regulates microvillar subdomains and structure. J Cell Biol. 2006; 175:803–813. [PubMed: 17145964]
14. Hillesheim J, Riederer B, Tuo B, Chen M, Manns M, Biber J, Yun C, Kocher O, Seidler U. Down regulation of small intestinal ion transport in PDZK1- (CAP70/NHERF3) deficient mice. Pflügers Arch. 2007; 454:575–586. [PubMed: 17347851]
15. Honegger KJ, Capuano P, Winter C, Bacic D, Stange G, Wagner CA, Biber J, Murer H, Hernando N. Regulation of sodium-proton exchanger isoform 3 (NHE3) by PKA and exchange protein

directly activated by cAMP (EPAC). Proc Natl Acad Sci U S A. 2006; 103:803–808. [PubMed: 16407144]

16. Kocher O, Pal R, Roberts M, Cirovic C, Gilchrist A. Targeted disruption of the PDZK1 gene by homologous recombination. Mol Cell Biol. 2003; 23:1175–1180. [PubMed: 12556478]
17. Lamprecht G, Seidler U. The emerging role of PDZ adapter proteins for regulation of intestinal ion transport. Am J Physiol Gastrointest Liver Physiol. 2006; 291:G766–G777. [PubMed: 16798722]
18. Lamprecht G, Weinman EJ, Yun CH. The role of NHERF and E3KARP in the cAMP-mediated inhibition of NHE3. J Biol Chem. 1998; 273:29972–29978. [PubMed: 9792717]
19. Lee-Kwon W, Kim JH, Choi JW, Kawano K, Cha B, Dartt DA, Zoukhri D, Donowitz M. Ca^{2+}-dependent inhibition of NHE3 requires PKC alpha which binds to E3KARP to decrease surface NHE3 containing plasma membrane complexes. Am J Physiol Cell Physiol. 2003; 285:C1527–C1536. [PubMed: 12954600]
20. Lee JH, Richter W, Namkung W, Kim KH, Kim E, Conti M, Lee MG. Dynamic regulation of cystic fibrosis transmembrane conductance regulator by competitive interactions of molecular adaptors. J Biol Chem. 2007; 282:10414–10422. [PubMed: 17244609]
21. Morales FC, Takahashi Y, Kreimann EL, Georgescu MM. Ezrin–radixin–moesin (ERM)-binding phosphoprotein 50 organizes ERM proteins at the apical membrane of polarized epithelia. Proc Natl Acad Sci U S A. 2004; 101:17705–17710. [PubMed: 15591354]
22. Murtazina R, Kovbasnjuk O, Zachos NC, Li X, Chen Y, Hubbard A, Hogema BM, Steplock D, Seidler U, Hoque KM, Tse CM, de Jonge HR, Weinman EJ, Donowitz M. Tissue-specific regulation of sodium/proton exchanger isoform 3 activity in Na^+/H^+ exchanger regulatory factor 1 (NHERF1) null mice. cAMP inhibition is differentially dependent on NHERF1 and exchange protein directly activated by cAMP in ileum versus proximal tubule. J Biol Chem. 2007; 282:25141–25151. [PubMed: 17580307]
23. Rossmann H, Jacob P, Baisch S, Hassoun R, Meier J, Natour D, Yahya K, Yun C, Biber J, Lackner KJ, Fiehn W, Gregor M, Seidler U, Lamprecht G. The CFTR associated protein CAP70 interacts with the apical $Cl^-/HCO3^-$ exchanger DRA in rabbit small intestinal mucosa. Biochemistry. 2005; 44:4477–4487. [PubMed: 15766278]
24. Saotome I, Curto M, McClatchey AI. Ezrin is essential for epithelial organization and villus morphogenesis in the developing intestine. Dev Cell. 2004; 6:855–864. [PubMed: 15177033]
25. Schultheis PJ, Clarke LL, Meneton P, Miller ML, Soleimani M, Gawenis LR, Riddle TM, Duffy JJ, Doetschman T, Wang T, Giebisch G, Aronson PS, Lorenz JN, Shull GE. Renal and intestinal absorptive defects in mice lacking the NHE3 Na^+/H^+ exchanger. Nat Genet. 1998; 19:282–285. [PubMed: 9662405]
26. Schweinfest CW, Spyropoulos DD, Henderson KW, Kim JH, Chapman JM, Barone S, Worrell RT, Wang Z, Soleimani M. slc26a3 (dra)-deficient mice display chloride-losing diarrhea, enhanced colonic proliferation, and distinct up-regulation of ion transporters in the colon. J Biol Chem. 2006; 281:37962–37971. [PubMed: 17001077]
27. Seidler U, Rottinghaus I, Hillesheim J, Chen M, Riederer B, Krabbenhoft A, Engelhardt R, Wiemann M, Wang Z, Barone S, Manns MP, Soleimani M. Sodium and chloride absorptive defects in the small intestine in Slc26a6 null mice. Pflügers Arch. 2008; 455:757–766. [PubMed: 17763866]
28. Sheng M, Sala C. PDZ domains and the organization of supramolecular complexes. Annu Rev Neurosci. 2001; 24:1–29. [PubMed: 11283303]
29. Shenolikar S, Voltz JW, Cunningham R, Weinman EJ. Regulation of ion transport by the NHERF family of PDZ proteins. Physiology (Bethesda). 2004; 19:362–369. [PubMed: 15546854]
30. Shenolikar S, Voltz JW, Minkoff CM, Wade JB, Weinman EJ. Targeted disruption of the mouse NHERF-1 gene promotes internalization of proximal tubule sodium-phosphate cotransporter type IIa and renal phosphate wasting. Proc Natl Acad Sci U S A. 2002; 99:11470–11475. [PubMed: 12169661]
31. Weinman EJ, Shenolikar S. The Na-H exchanger regulatory factor. Exp Nephrol. 1997; 5:449–452. [PubMed: 9438172]

32. Weinman EJ, Steplock D, Shenolikar S. NHERF-1 uniquely transduces the cAMP signals that inhibit sodium-hydrogen exchange in mouse renal apical membranes. FEBS Lett. 2003; 536:141–144. [PubMed: 12586353]

33. Weinman EJ, Steplock D, Wang Y, Shenolikar S. Characterization of a protein cofactor that mediates protein kinase A regulation of the renal brush border membrane Na^+–H^+ exchanger. J Clin Invest. 1995; 95:2143–2149. [PubMed: 7738182]

34. Yun CH, Oh S, Zizak M, Steplock D, Tsao S, Tse CM, Weinman EJ, Donowitz M. cAMP-mediated inhibition of the epithelial brush border Na^+/H^+ exchanger, NHE3, requires an associated regulatory protein. Proc Natl Acad Sci U S A. 1997; 94:3010–3015. [PubMed: 9096337]

35. Zachos NC, Tse M, Donowitz M. Molecular physiology of intestinal Na^+/H^+ exchange. Annu Rev Physiol. 2005; 67:411–443. [PubMed: 15709964]

36. Zizak M, Lamprecht G, Steplock D, Tariq N, Shenolikar S, Donowitz M, Yun CH, Weinman EJ. cAMP-induced phosphorylation and inhibition of Na^+/H^+ exchanger 3 (NHE3) are dependent on the presence but not the phosphorylation of NHE regulatory factor. J Biol Chem. 1999; 274:24753–24758. [PubMed: 10455146]

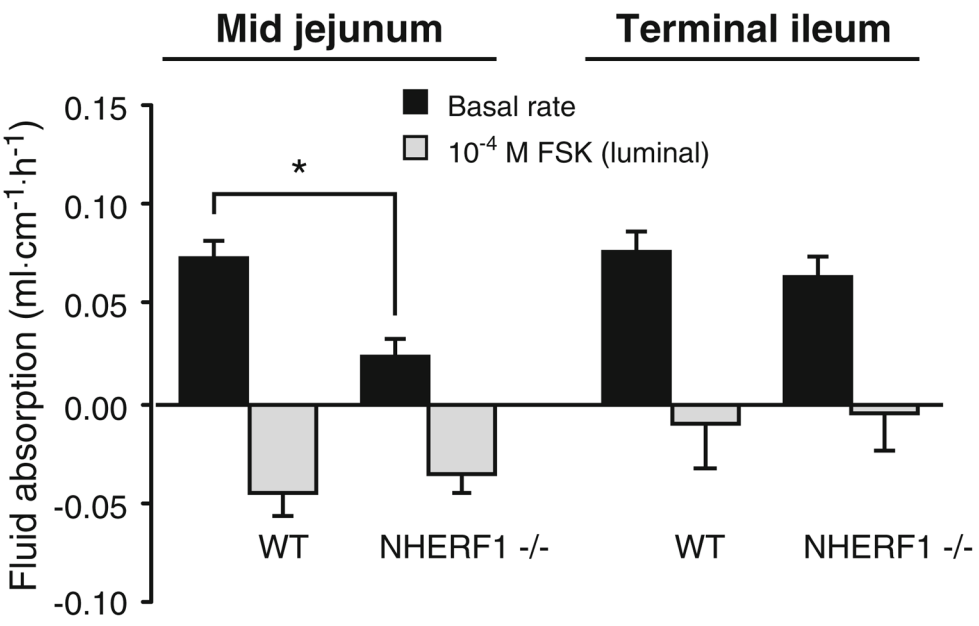

Fig. 1.

Fluid transport in the basal state and after FSK stimulation in the jejunum and ileum of anesthetized NHERF1$^{+/+}$ and NHERF1$^{-/-}$mice in vivo. Approximately 5 cm of jejunum (*left*) or ileum (*right*) was perfused for 30 min and the amount of fluid absorbed was measured at the end of the experiment. *Positive numbers* indicate that fluid was absorbed and *negative numbers* denote secretion. The fluid absorption rate in the basal state in NHERF1 null mice was significantly reduced in the jejunum, but not in the ileum (*black bars*, * $p<0.05$). In addition, the change in jejunal fluid transport from absorption to secretion was significantly less in the NHERF1-deficient mice than the WT mice (*gray bars*). Data represent values from five independent experiments and are expressed as mean ±SE

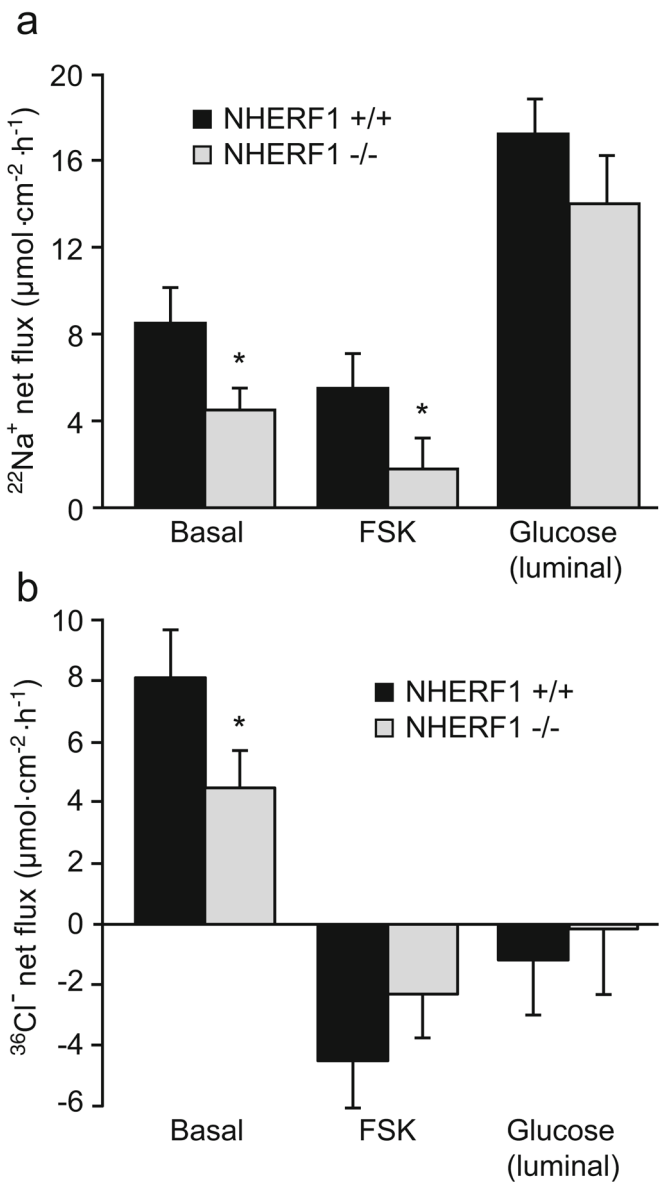

Fig. 2.

Net $^{22}Na^+$ (**a**) and $^{36}Cl^-$ (**b**) fluxes in isolated NHERF1$^{+/+}$ and NHERF1$^{-/-}$ midjejunal mucosa. Fluxes were calculated by subtraction of the individual serosal to mucosal flux values from the mucosal to serosal fluxes for each paired tissue sample as determined in NHERF1$^{+/+}$ (*black bars*) and NHERF1$^{-/-}$ mice (*gray bars*). Measurements were performed in the basal state and after the addition of 10^{-5} M FSK or 25 mM glucose, as indicated. Basal as well as FSK-inhibited Na^+ absorption was reduced in NHERF1$^{-/-}$ mice (*p<0.05), but the relative inhibition by FSK was similar. The response to 25 mM luminal glucose, added to stimulate the Na^+–glucose cotransporter, was similar (n=9). The net $^{36}Cl^-$ flux was reduced in the basal state of NHERF1$^{-/-}$ jejunum, and the effect of FSK on the flux change was diminished. I_{sc} values are given in the text (n=8)

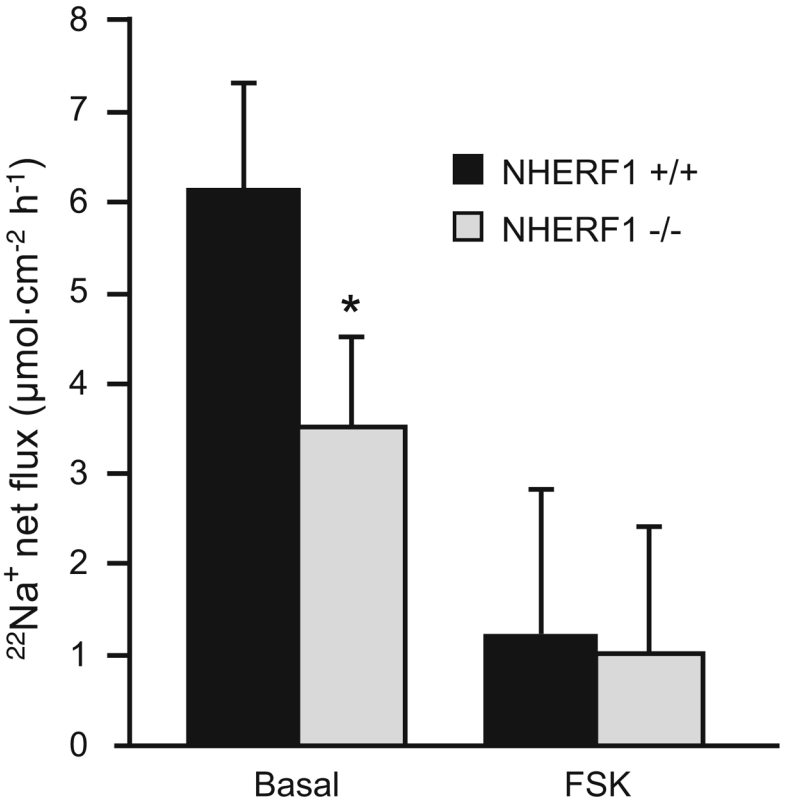

Fig. 3.

Net $^{22}Na^+$ flux in isolated NHERF1$^{+/+}$ and NHERF1$^{-/-}$proximal colonic mucosa. The net $^{22}Na^+$ flux in colonic mucosa from NHERF1$^{-/-}$ mice (*gray bars*) was significantly reduced compared with NHERF1$^{+/+}$ littermates (*black bars*; *p<0.05); 10^{-5} M FSK in the serosal compartment reduced the absorption in both NHERF1$^{+/+}$ and NHERF1$^{-/-}$ mucosa (n=9)

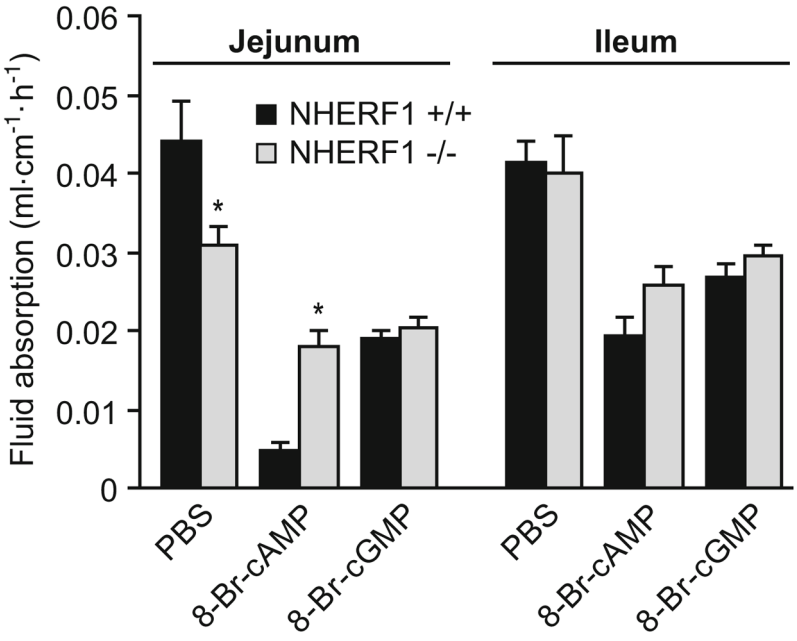

Fig. 4.

Closed loop experiments confirm segmental differences in absorptive rates in NHERF1$^{+/+}$ and NHERF1$^{-/-}$ mice. Fluid absorption was measured simultaneously in closed intestinal loops from the jejunum and ileum of the same mouse. In the jejunum, but not in the ileum, fluid absorption was reduced in the NHERF1-deficient mice, and the inhibition of absorption by the cAMP analog was attenuated. n=8; *p<0.05

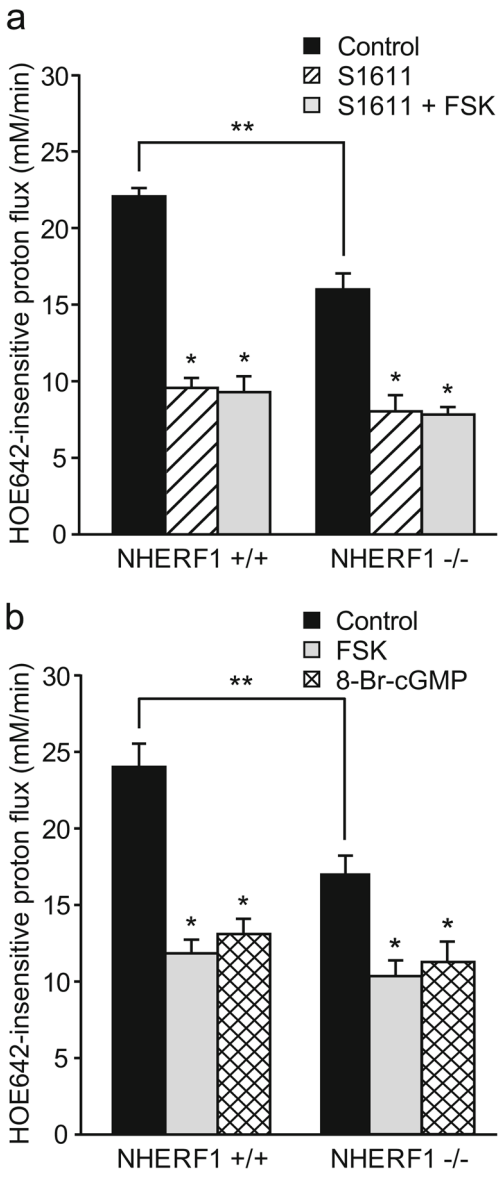

Fig. 5.

Fluorometric assessment of NHE3 activity in surface enterocytes. The HOE642-insensitive, Na^+-dependent acid-activated proton flux was measured in BCECF-loaded cells of the cryptal opening from isolated colonic crypts of $NHERF1^{+/+}$ and $NHERF1^{-/-}$ mice. **a** In $NHERF1^{-/-}$surface enterocytes, the HOE642-insensitive proton flux was significantly reduced (**p<0.05). Furthermore, this significant reduction of the HOE642-insensitive, Na^+-dependent, acid-activated proton flux rates was observed in the absence but not the presence of 10 μM S1611 (*p<0.05), indicating a reduction of NHE3 activity. In the presence of S1611, FSK did not exert an additional inhibitory effect, indicating that the inhibitory effect of FSK on the proton flux was due to NHE3 inhibition (n=6). **b** Both 10^{-5} M FSK and 2×10^{-4} M 8-Br-cGMP significantly inhibited acid-activated proton efflux rates in $NHERF1^{+/+}$ and $NHERF1^{-/-}$ colonocytes (*p<0.05 vs. control; n=6)

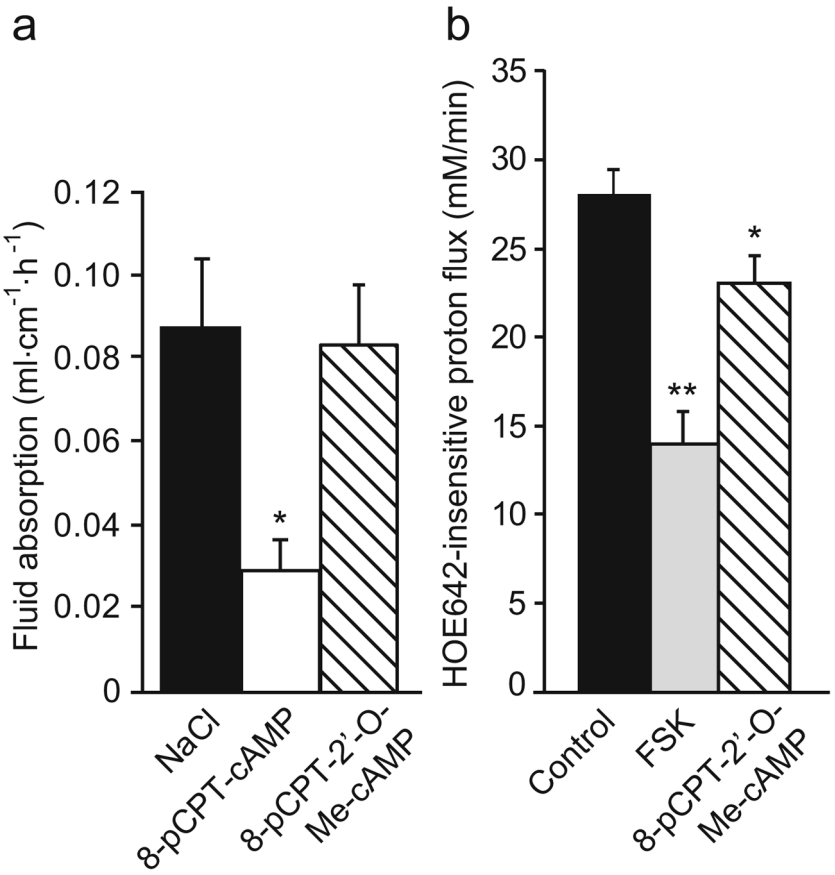

Fig. 6.

Effect of EPAC activation on jejunal fluid absorption and surface colonocyte NHE3 activity in WT mice. **a** Whereas 200 μM 8-pCPT-cAMP caused a significant inhibition of jejunal fluid absorption (*p<0.05), the same concentration of the structurally related selective EPAC activator 8-pCPT-2′-*O*-Me-cAMP had no effect (n=5). **b** In surface colonocytes, 100 μM 8-pCPT-2′-*O*-Me-cAMP had a small but significant inhibitory effect on the proton flux (*p<0.05), but full activation of adenylate cyclase by FSK caused a much more pronounced inhibition (**p<0.05; n=6)

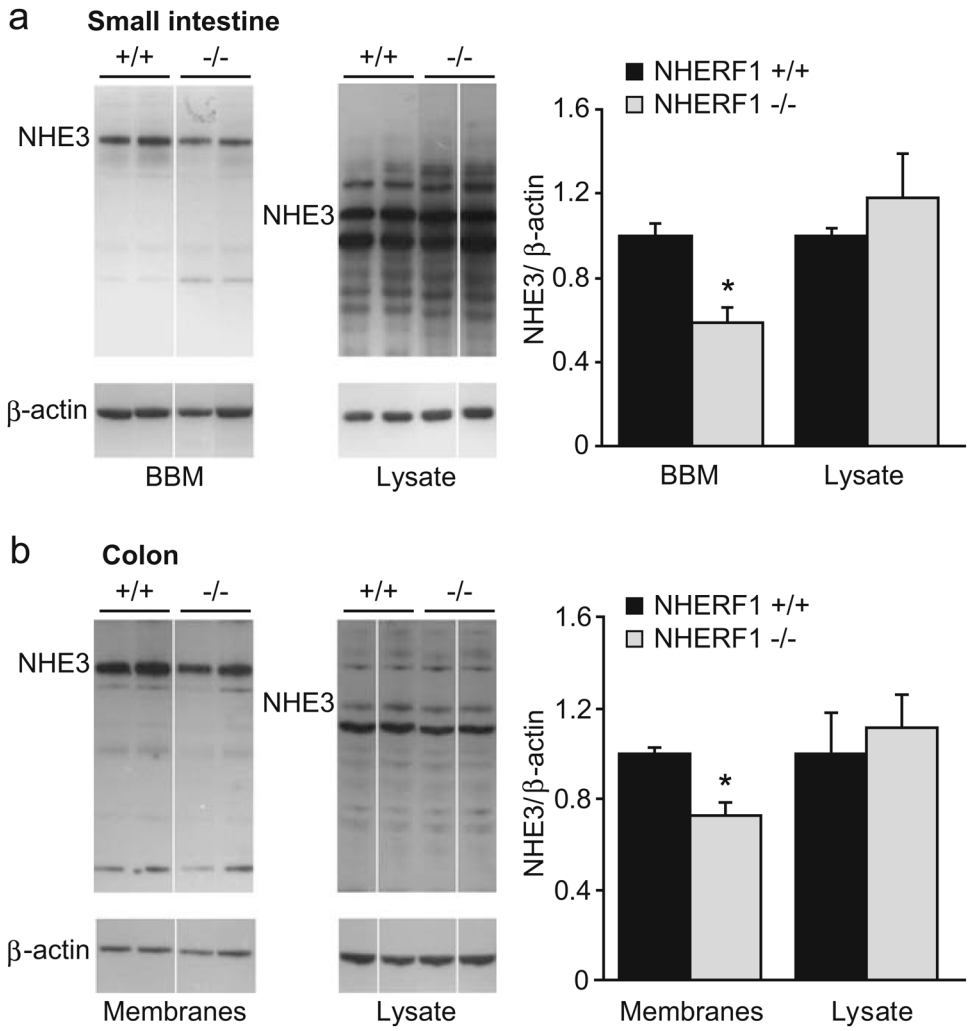

Fig. 7.

Western blot analysis of NHE3 protein in the BBM and the enterocyte lysate from small and large intestine of NHERF1$^{+/+}$ and NHERF1$^{-/-}$mice. **a** NHE3 protein abundance was significantly reduced in BBM preparations from the small intestine from NHERF1$^{-/-}$mice (*gray bars*, n=11) compared with WT littermates (*black bars*, n=19, *p<0.05), whereas no difference was seen in the enterocyte lysates (n=7). Representative examples of Western blots are shown at the *left* and the average intensities of NHE3 (relative to β-actin) are shown in the bar graph. **b** Similar results were obtained in the colon (n=4–6)

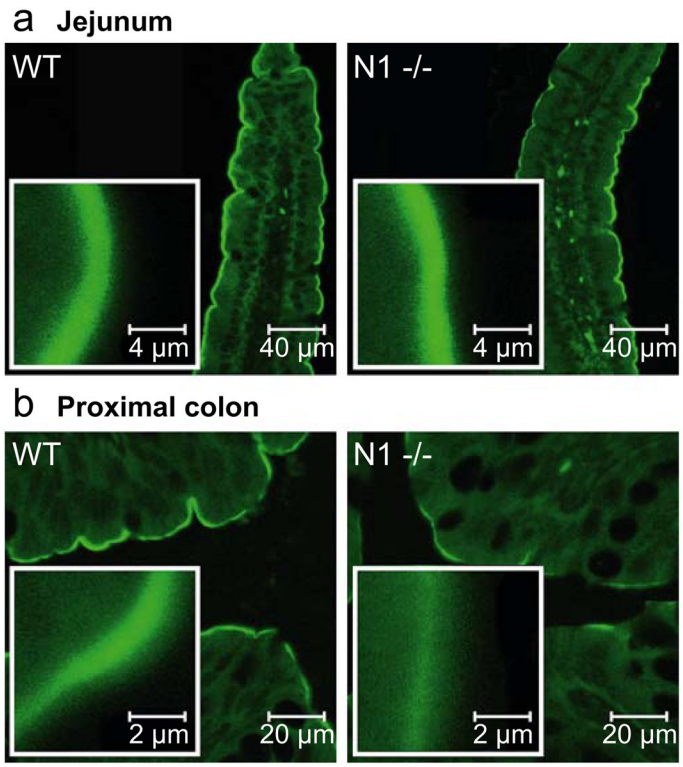

Fig. 8.

Immunohistochemical NHE3 staining reveals normal localization of NHE3 in jejunal and colonic apical membrane of NHERF1$^{-/-}$mice. The NHE3 localization at the apical border of the jejunum (**a**) and colon (**b**) was qualitatively similar in WT (*left panels*) and NHERF1$^{-/-}$ (*right panels*) mice with considerable variability in the signal intensity within each group of mice. Images are representative examples from five independent experiments using tissue from three different mouse couples. Inserts show a ×10 magnification of a part from the image shown in the larger panels

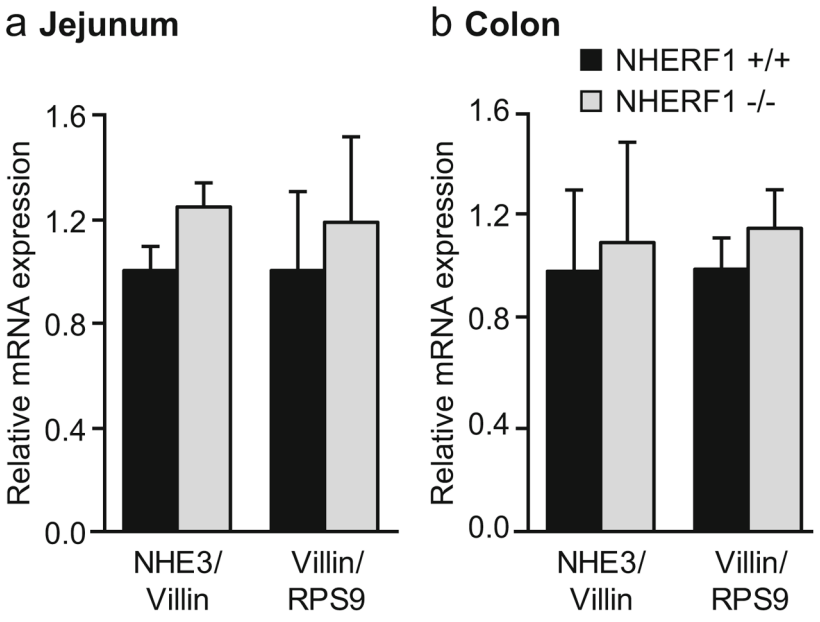

Fig. 9.

Expression of NHE3 and villin mRNA determined by quantitative RT-PCR. No changes in NHE3 mRNA expression levels (relative to the structural brush border protein villin) were observed between NHERF1 $^{+/+}$ and NHERF1$^{-/-}$ in the small (**a**) and large (**b**) intestine. In addition, no changes in villin expression levels (relative to the ribosomal protein RPS9) were observed in NHERF1$^{-/-}$ mice compared with WT mice. Data represent average values from three separate measurements in three pairs of NHERF1$^{+/+}$ and NHERF1$^{-/-}$mice. The expression levels in the NHERF1$^{-/-}$ tissues are relative to the WT expression set at 1

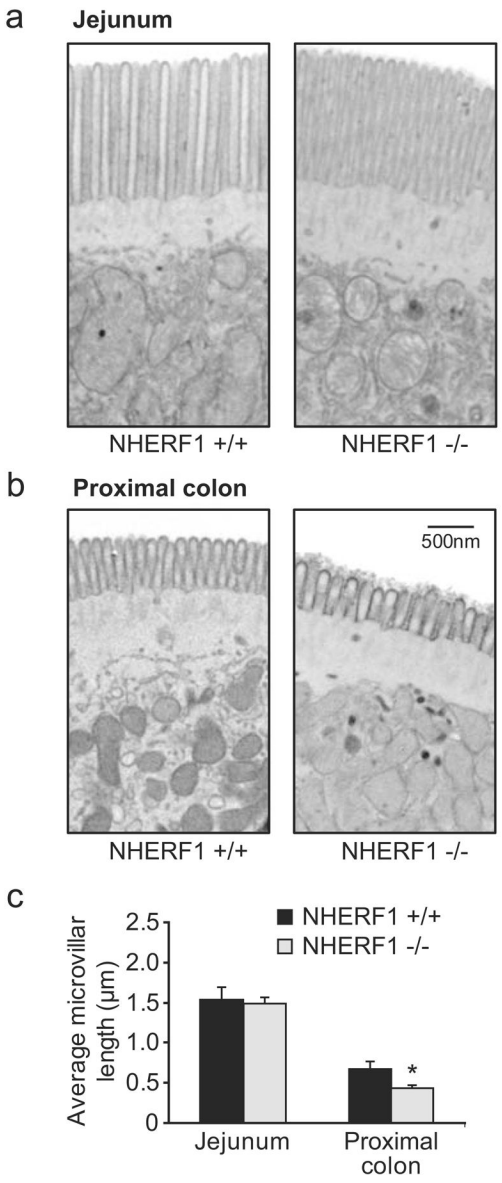

Fig. 10.

Reduced microvillar length in the colon but not in the jejunum of NHERF1 null mice. **a** The ultrastructure of jejunal enterocytes from NHERF1 null mice and WT controls was indistinguishable. **b** In contrast, the microvilli from colonic enterocytes from NHERF1-deficient mice (*right panel*) were significantly shortened. Images are representative examples of sections made from three age-and sex-matched mice in each group

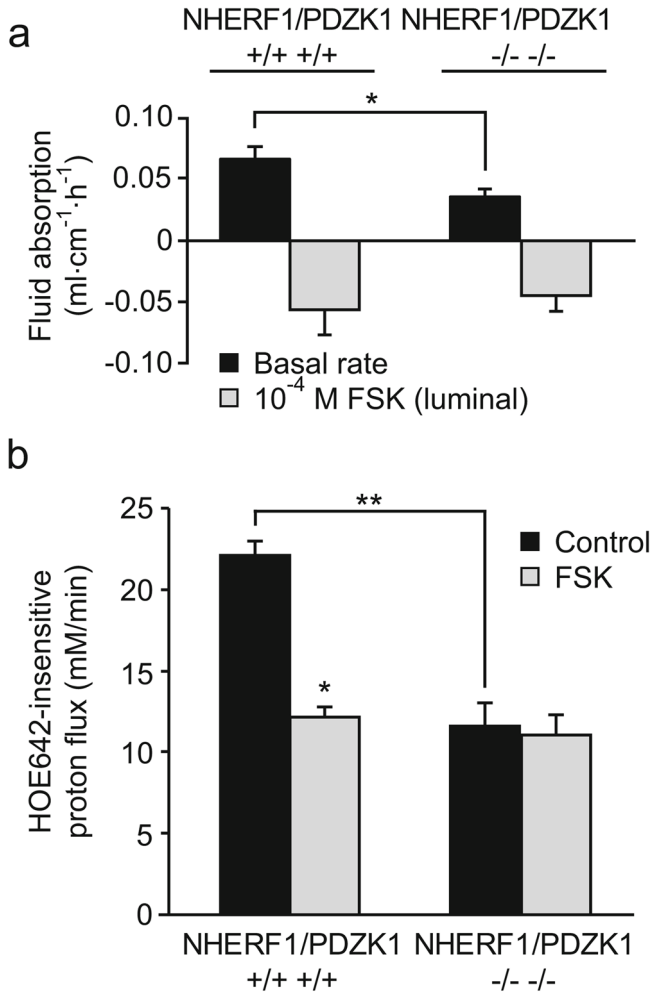

Fig. 11.

In vivo jejunal fluid movement and NHE3 activity in surface colonocytes in NHERF1/PDZK1 double-deficient mice. **a** Fluid absorption under basal conditions (*black bars*) and in the presence of FSK (*gray bars*) was determined in NHERF1/PDZK1$^{-/-}$ jejunum. The reduced basal fluid absorption (p<0.05) and the reduced response to FSK was similar to what was observed in the NHERF1$^{-/-}$ jejunum as shown in Fig. 1a (n=5). **b** In contrast, the reduction of the basal acid-activated NHE3 transport rate (*black bars*) in colon surface enterocytes was significantly larger (**p<0.05) in NHERF1/PDZK1 double-deficient mice than in NHERF1-deficient mice (see Fig. 5). Furthermore, inhibition by FSK was completely abrogated (n=6)